Desalination and Water Treatment
www.deswater.com

doi: 10.1080/19443994.2016.1140680

57 (2016) 24352–24358
November

Taylor & Francis
Taylor & Francis Group

Degradation of Reactive Blue 19 using advanced oxidation methods: gliding-arc plasma discharge

Bassam AlHamad*, Nader Al-Bastaki

Department of Chemical Engineering, College of Engineering, University of Bahrain, P.O. Box 32038, Isa Town, Bahrain, Tel. +973 17438088; Fax: +973 17449658; email: balhamad@uob.edu.bh (B. AlHamad), Tel. +973 17876622; Fax: +973 17449658; email: nalbastaki@uob.edu.bh (N. Al-Bastaki)

Received 5 July 2015; Accepted 5 January 2016

ABSTRACT

Aqueous solutions of Reactive Blue 19 (RB19) were treated using advanced oxidation process (AOP) to remove the color from the water. The AOP process was applied using a non-thermal gliding-arc plasma discharge with and without the addition of hydrogen peroxide, H_2O_2, to the samples. The gliding-arc experiments were conducted in an open reactor using humid compressed air. Treating 20-ppm solutions without using H_2O_2 was successful in reducing the RB19 concentration but resulted in the increase of a secondary byproduct. With the use of H_2O_2, a higher RB19 removal rate was achieved and the byproduct production was avoided. The pH and conductivity measurements indicated the presence of a higher rate of reactive species when H_2O_2 was used. By treatment of the samples for 60 min, an RB19 removal rate of 87% was achieved when no H_2O_2 was used and an RB19 removal rate of 98.9% was achieved when H_2O_2 was added. Samples treated without the addition of H_2O_2 exhibited an additional post-discharge reaction in the case of samples exposed to only 10 and 20 min of treatment with the plasma discharge. Measurements taken for up to three hours of post discharge for the samples treated for 10 min with plasma discharge showed additional RB19 removed from 26.9% at 0 min post discharge to 59.6% at 180 min post discharge. Similarly, for the sample exposed to 20 min of plasma discharge, the RB19 removal rate increased from 67.2 to 78.6%. Samples treated for longer periods did not exhibit significant post-discharge effects.

Keywords: Water treatment; Advanced oxidation; Non-thermal gliding-arc plasma discharge; Post-discharge reaction; Dye treatment

1. Introduction

Contamination of the water resources with hazardous pollutants is a major concern that can seriously threat the health and well-being of many communities around the world. Organic pollutants are produced in many industries and end up in the effluent water in spite of various degrees of treatment. Advanced oxidation techniques, such as atmospheric plasma [1–10], photocatalysis, ozonation, and electrochemical degradation [11–24], have provided an alternative solution for removing these pollutants. Atmospheric plasma has been used in removing organics and colors under different conditions [1–10,25–28]. The list of active species is discussed in Refs [29,30]. Merouni et al. [8]

*Corresponding author.

used gliding-arc plasma discharge to treat Alizarin Red S in the presence of peroxinitrite. They also evaluated the effects of continued post-discharge reactions after stopping the plasma discharge due to the presence of reactive species produced during the discharge period. They evaluated the additional color removal achieved during the post-discharge period. Post-discharge effects in atmospheric plasma were also observed and studied in a number of recent works [8,26,28,29].

Benstaali et al. [2] compared the effectiveness of degradation of methyl orange (MO) in aqueous solutions using non-thermal humid air plasma produced by gliding-arc discharges with and without TiO_2 catalyst and H_2O_2 and combinations of both. They found that the treatment without the TiO_2 and H_2O_2 removed the MO but a structure with a single aromatic ring was produced as a result of the cleavage of the MO molecule. They reported that adding TiO_2 to the solution treated with plasma did not result in any improvement, while adding H_2O_2 resulted in the removal of the secondary compound as well as the original MO. Benetoli et al. [1] used pyrite as a catalyst for the degradation of methylene blue (MB) in aqueous solutions using non-thermal plasma using three gasses, namely, O_2, N_2, and Ar. They reported that adding pyrite catalyst in acid medium resulted in a substantial enhancement of the dye removal. Jiang et al. [6] studied the degradation of MO using non-thermal plasma in a circulatory airtight reactor and found that the energy efficiency was enhanced using the airtight reactor. They observed that the degradation efficiency depended on the sample volume and concentration. Other types of atmospheric plasma process have also been used to degrade dyes such as pulsed discharge plasma [7] and dielectric barrier discharge (DBD) plasma [5,9,10]. Jin et al. [7] studied the operating parameters for decolorization of MB and MO dye by pulsed discharged plasma in water using response surface methodology. Huang et al. [5] studied the degradation of MB using DBD plasma. They analyzed the radical species present in the gas and liquid phases and proposed a mechanism for the degradation of MB using the bond dissociation energy theory. Reddy et al. [9] showed that DBD non-thermal plasma was effective in removing MB dye and they studies the effect of various parameters on the process including the applied voltage, gas flow rate, concentration of the dye, and addition of Na_2SO_4 and Fe^{2+} catalyst. Tichonovas et al. [10] investigated the degradation of a variety of industrial textile dyes in a pilot DBD semi-continuously operated plasma reactor. They reported that 10 of the 13 dyes that were studied decomposed up to 95% within 300 sec. Dojčinović et al. [3] studied the decolorization of four reactive textile dyes using water falling film DBD. They investigated the effects of addition of different catalysts (H_2O_2, Fe^{2+} and Cu^{2+}) on the decolorization during subsequent recirculation of dye solution through the DBD reactor. Doubla et al. [4] studied the plasma-chemical decolorization of bromothymol blue by gliding electric discharge at atmospheric pressure. Rajkumar et al. [11] studied the electrochemical degradation of Reactive Blue 19 in chloride medium for the treatment of textile-dyeing wastewater with identification of intermediate compounds. He et al. [13] used ozonation combined with sonolysis to mineralize Reactive Blue 19 and studied the performance and mechanism of the degradation process.

In general, these studies indicate that atmospheric non-thermal plasma is a very promising process for removal of colors, but the process requires more investigation to optimize the degradation of the original dye and the side products that may be produced as a result of the cleavage of the original organic molecule. Several reactive species have been suggested to be present in the gliding-arc discharge, including free radicals and ionic species, such as $^{\cdot}OH$, $^{\cdot}NO$, $^{\cdot}O$, $HO_2^{\cdot}$, $H^{\cdot}$, O_3, H_2O_2, O_2^+, O^+, N^+, etc. [1]. Brisset and Hnatiuc [30] discussed the main compounds of non-thermal plasmas generated by a discharge in humid air at atmospheric pressure and their effective oxidizing and acidic properties in aqueous waste solutions. They attributed the acid effects to transient nitrous and peroxynitrous acids and to stable nitric acid while the oxidizing effect was attributed to H_2O_2 provided by the dimer formation of hydroxyl radicals, $OH^{\cdot}$, and also to peroxynitrous acid ONOOH and its salt which are involved in the oxidation process of nitrous to nitric acid.

Delayed or post-discharge reactions have been the subject of some of recent papers. Brisset at al. [26] discussed the temporal post-discharge reactions which occur when the target is no longer exposed to the non-thermal gliding-arc plasma. They suggested that the post-discharge treatment has a role in improving the efficiency of water treatment using the plasma-discharge process. Laminsi et al. [28] studied the effect of direct treatment of Fe^{II} complexes aqueous solutions with non-thermal gliding-arc plasma in a closed reactor and the post-exposure effects after removing the samples from the plasma reactor. Brisset and Pawlat [29] studied the non-thermal gliding-arc plasma-discharge and post-discharge reactions. They discussed the chemical interaction between non-thermal plasma species and aqueous solutions with emphasis on the oxidizing and acidic effects resulting from formed peroxynitrite ONOO– and derived species, such as

transient nitrite and stable HNO_3. Merouni et al. [8] investigated influence of peroxinitrite in gliding-arc discharge treatment of Alizarin Red S and post-discharge effects. They suggested that the process cost can be reduced using a short-discharge exposure time followed by a longer post-discharge time during which additional reactions continue, driven by the active species generated during the discharge period, particularly peroxynitrite.

The objectives of the current work were to study the effect of exposure time on the degradation of the RB19 color, and to study the possibility of enhancing the degradation of the RB19 color by adding H_2O_2. Another objective was to study effect of possible continued reactions during the post-discharge period, exhibited by additional RB19 removal.

2. Experimental setup and procedures

2.1. Gliding-arc non-thermal plasma-discharge reactor

The experimental setup for the gliding-arc non-thermal discharge plasma rector used in the current work was described by [2]. Fig. 1 shows a schematic diagram of the experimental setup and Fig. 2 shows a photograph of the gliding-arc plasma generator. Air from a compressed air cylinder is passed though distilled water and flows through a nozzle through two semi-elliptical electrodes supplied with a 220 V/10 kV high-voltage Aupem Sefli transformer [2]. The mean operating conditions are 160 mA and 600 V in working conditions. An electric arc is generated between the electrodes at the upper end of the gap between the two electrodes, where the gap is smallest [2]. As the humid air flow is started, the electric arc moves down the increasing electrodes gap before breaking at the arc-length threshold. The air flow rate is measured using Show Rate Brooks rotameter.

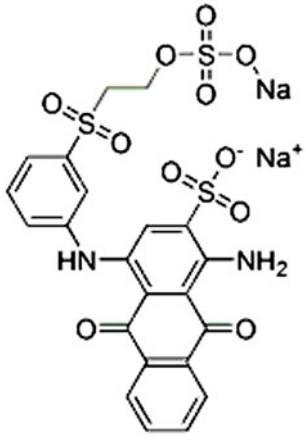

Fig. 1. Chemical structure of Reactive Blue 19 (www.chemicalbook.com).

2.2. Sample preparation and non-thermal plasma experimental procedures

The Reactive Blue 19 (RB19) dye, with a formula of $C_{22}H_{16}N_2Na_2O_{11}S_3$, a molecular mass of 626.54 g/mol and a CAS No. 2580-78-1, was supplied by Town End, Plc, Leeds, UK. RB19 has a rather complex structure and is characterized by the presence of anthraquinone structure as shown in Fig. 1.

The RB19 powder was dissolved in distilled water to prepare 20 ppm concentration. Hydrogen peroxide (30% aqueous solution) was supplied by VWR International. The experiments were conducted either without H_2O_2 or with the addition of 1 ml of the H_2O_2 solution to the 130 ml mixture.

A magnetically stirred sample was placed at a distance of 7.5 cm from the ignition point of the electrical arc and treated by a non-thermal plasma of humid air at flow rates of 2.5 L min^{-1}. The gliding-arc works in an open reactor. Samples were taken for analysis every 5 min. Absorbance measurements were carried out using a Schimadzu UV–vis spectrophotometer model UV-1800. Measurements of pH were carried out using a Trans Instruments BP3001 Professional Benchtop pH meter. Conductivity measurements were taken using a WTW Multi 350i conductivity meter (Fig. 3).

3. Results and discussion

When the samples were treated with gliding-arc plasma, substantial reduction in the RB19 concentration was achieved up to an exposure time of 30 min, as exhibited by the absorption of the peak at 591 nm. Further drops beyond this exposure time were very limited. This may indicate that equilibrium has been achieved at the current experimental conditions. It can be noticed on Fig. 4 that the peak at 369 nm increases with exposure time, which could be ascribed to a diazo intermediate.

The variations of these two peaks with exposure time are also shown in Fig. 5. These results show a maximum of about 87% removal of the RB19. The results show that the absorbance of the RB19 decreases, and that the removal rate does not significantly change after 30 min of exposure. Fig. 6. shows that while the conductivity of the exposed sample keeps increasing beyond 30 min, the pH virtually stays unchanged after 30 min of exposure. This may

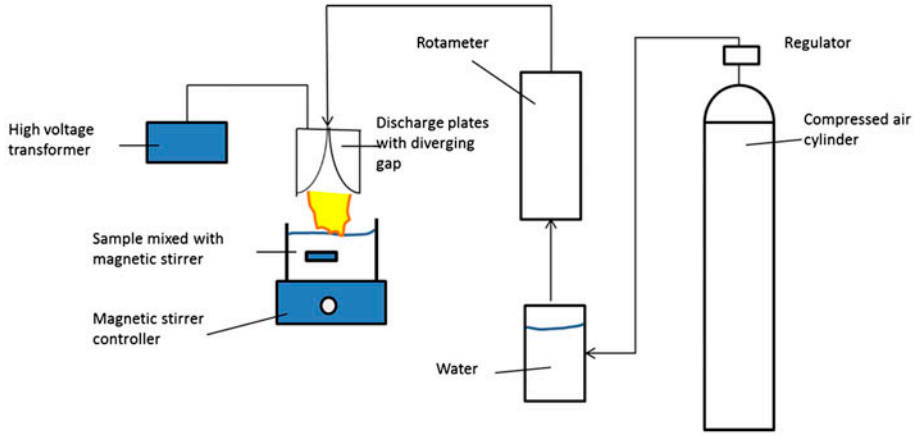

Fig. 2. A schematic diagram of the experimental setup.

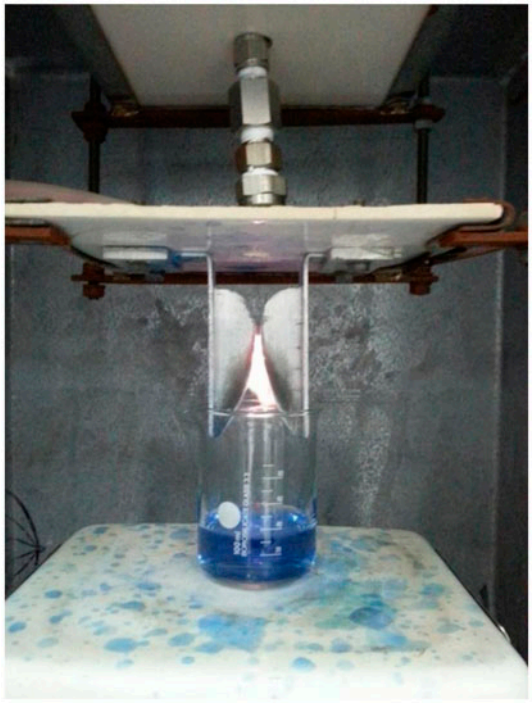

Fig. 3. A photograph of the gliding-arc plasma apparatus.

indicate the concentration of acidic species remain almost constant at the equilibrium value achieved at 30 min. The increase in conductivity is attributed to the incorporation of N-containing ions (first nitrite, then peroxynitrite and its isomer, nitrate) [29]. The acid effect is attributed to HONO and the formation of N-containing species to the occurrence of ONOOH which acts as a source of nitrosonium involved in the reaction with amino groups [29].

As discussed earlier, Merouni et al. [8], Brisset et al. [26,29], and Laminsi et al. [28] observed and

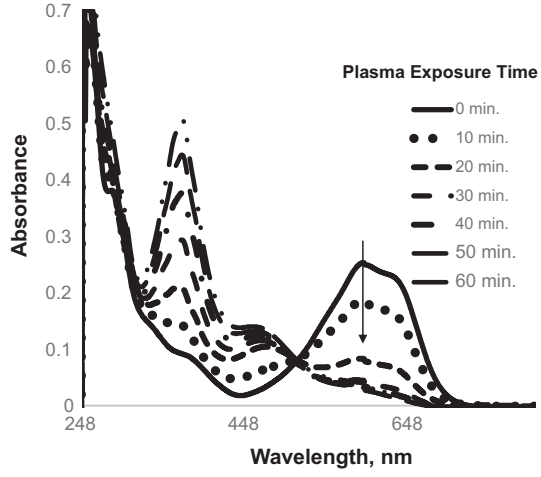

Fig. 4. Absorbance spectra at different gliding-arc plasma exposure times for 20 ppm RB19 with no H_2O_2 added.

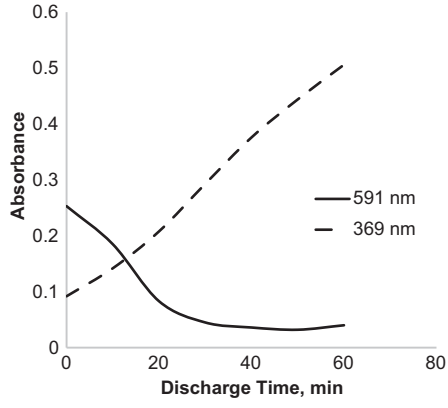

Fig. 5. Drop in RB19 (591 nm) and increase in intermediate side product peak (369 nm) absorbances with plasma exposure time.

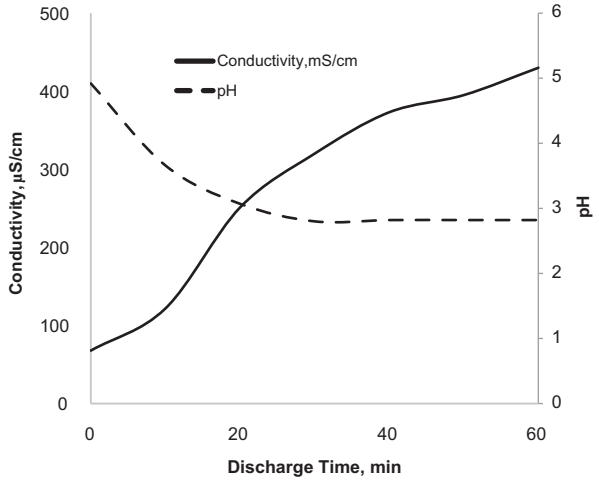

Fig. 6. Variation of conductivity and pH of the sample with glide plasma exposure time.

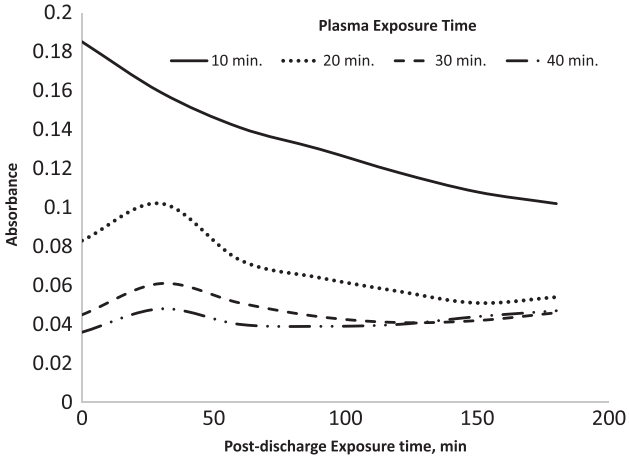

Fig. 7. Absorbance at 591 nm for samples exposed to plasma for different periods and measured immediately after removal and at every 30 min after that.

measured post-discharge effects after stopping the exposure to the plasma. For the current work, samples exposed to different discharge times were kept to observe any further reactions during the post-discharge period. For the post-discharge period, the absorbance was measured up to a post-discharge period of three hours. The results of the post-discharge measurements absorbance of RB19 are shown in Fig. 7. These results show that further removal of RB19 was achieved for samples exposed to discharge periods of 10 and 20 min. A very small post-discharge removal is noticed for the sample exposed to the discharge of 30 min, and very little removal was noticed for the samples exposed to longer discharge periods. For the sample treated with 10 min of glide-arc plasma, an RB19 removal of 26.9% was achieved and at the end of the three hours of post discharge, the removal of RB19 increased to 59.6%. Similarly, for the sample exposed to at 20 min, an RB19 removal of 67.2% was achieved, and at the end of three hours of post discharge, the removal reached 78.6%. Samples treated with glide-arc non-thermal plasma for longer periods did not exhibit significant post-discharge effects.

In order to enhance the removal rate of RB19 by gliding-arc plasma treatment, 1 ml of H_2O_2 was added to the sample. The results of these tests are shown in Fig. 8 and Table 1. Table 1 shows that up to 98.9% of

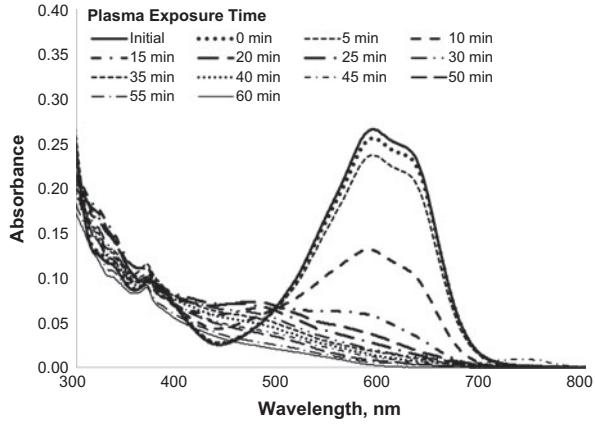

Fig. 8. Absorbance spectra variations with treatment time for RB19 samples with 1 ml H_2O_2 exposed to non-thermal gliding-arc plasma.

Table 1
Removal rate and absorbances of RB19 at 591 nm for samples with 1 ml H_2O_2

Time (min)	Removal (%)	Absorbance
0	0.00	0.266
5	3.76	0.256
10	10.90	0.237
15	50.75	0.131
20	78.57	0.057
25	86.47	0.036
30	89.85	0.027
35	92.48	0.02
40	93.23	0.018
45	94.74	0.014
50	95.49	0.012
55	96.99	0.008
60	97.74	0.006
65	98.87	0.003

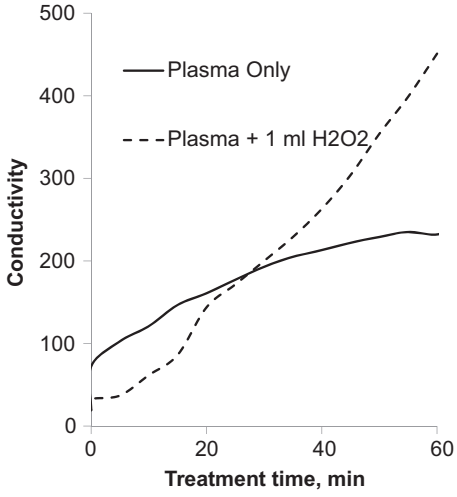

Fig. 9. Comparison of the change in the solution conductivity with treatment time for the samples with and without the addition of H_2O_2.

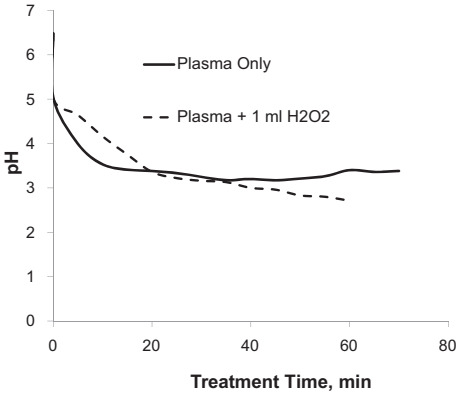

Fig. 10. Comparison of the change in the pH of the solution with treatment time, between the samples with and without the addition of H_2O_2.

RB19 has been removed. The peak at 369 nm is also reduced significantly. Fig. 9 shows that the increase in the conductivity for the samples in which H_2O_2 was added was much higher. This may indicate a higher production rate of the reactive species, which is correlated to the higher dye removal rate. Fig. 10 also shows that the drop rate in the pH for sample that contained H_2O_2 was higher, which is an observation that is consistent with the previous argument.

4. Conclusions

Treating 20-ppm solutions without using H_2O_2 was successful in reducing the RB19 concentration but resulted in the increase of a secondary byproduct. With the use of H_2O_2, a higher RB19 removal rate was achieved and the byproduct production was avoided. The pH and conductivity measurements indicated the presence of a higher rate of reactive species when H_2O_2 was used. By treatment of the samples for 60 min, an RB19 removal rate of 87% was achieved when no H_2O_2 was used; however, with samples mixed with 1 ml of H_2O_2, an RB19 removal rate of 98.9% was achieved. Samples treated without the addition of H_2O_2 exhibited an additional post-discharge reaction for samples exposed to only 10 and 20 min of treatment with the plasma discharge. Measurements taken for up to three hours of post discharge for the sample exposed to 10 min of treatment showed additional RB19 removal from 26.9% at 0 min of post discharge to 59.6% at 180 min of post discharge. Similarly, for the sample treated with plasma discharge for 20 min, the RB19 removal rate increased from 67.2 to 78.6%. Samples treated for longer periods did not exhibit significant post-discharge effects.

References

[1] L.O. Benetoli, B.M. Cadorin, V.Z. Baldissarelli, R. Geremias, I.G.d. Souza, N.A. Debacher, Pyrite-enhanced methylene blue degradation in non-thermal plasma water treatment reactor, J. Hazard. Mater. 237–238 (2012) 55–62.
[2] B. Benstaali, N. Al-Bastaki, A. Addou, J.L. Brisset, Plasma-chemical and photo-catalytic degradation of Methyl Orange, Int. J. Environ. Waste Manage. 11 (2013) 157–177.
[3] B.P. Dojčinović, G.M. Roglić, B.M. Obradović, M.M. Kuraica, M.M. Kostić, J. Nešić, D.D. Manojlović, Decolorization of reactive textile dyes using water falling film dielectric barrier discharge, J. Hazard. Mater. 192 (2011) 763–771.
[4] A. Doubla, L.B. Boubabello, M. Fotso, J.-L. Brisset, Plasmachemical decolourisation of Bromothymol Blue by gliding electric discharge at atmospheric pressure, Dyes Pigm. 77 (2008) 118–124.
[5] F. Huang, L. Chen, H. Wang, Z. Yan, Analysis of the degradation mechanism of methylene blue by atmospheric pressure dielectric barrier discharge plasma, Chem. Eng. J. 162 (2010) 250–256.
[6] B. Jiang, J. Zheng, Q. Liu, M. Wu, Degradation of azo dye using non-thermal plasma advanced oxidation process in a circulatory airtight reactor system, Chem. Eng. J. 204–206 (2012) 32–39.
[7] Y. Jin, Y. Wu, J. Cao, Y. Wu, Optimizing decolorization of Methylene Blue and Methyl Orange dye by pulsed discharged plasma in water using response surface methodology, J. Taiwan Inst. Chem. Eng. 45 (2014) 589–595.
[8] D.R. Merouni, F. Abdelmalek, M.R. Chezzar, A. Semmoud, A. Addou, J.I. Brisset, Influence of peroxinitrilte in gliding arc discharge treatment of alizarin Red S and postdischarge effects, Ind. Eng. Chem. Res. 52 (2013) 1471–1480.

[9] P.M.K. Reddy, B.R. Raju, J. Karuppiah, E.L. Reddy, C. Subrahmanyam, Degradation and mineralization of methylene blue by dielectric barrier discharge non-thermal plasma reactor, Chem. Eng. J. 217 (2013) 41–47.
[10] M. Tichonovas, E. Krugly, V. Racys, R. Hippler, V. Kauneliene, I. Stasiulaitiene, D. Martuzevicius, Degradation of various textile dyes as wastewater pollutants under dielectric barrier discharge plasma treatment, Chem. Eng. J. 229 (2013) 9–19.
[11] D. Rajkumar, B.J. Song, J.G. Kim, Electrochemical degradation of Reactive Blue 19 in chloride medium for the treatment of textile dyeing wastewater with identification of intermediate compounds, Dyes Pigm. 72 (2007) 1–7.
[12] S. Haji, B. Benstaali, N. Al-Bastaki, Degradation of methyl orange by UV/H_2O_2 advanced oxidation process, Chem. Eng. J. 168 (2011) 134–139.
[13] Z. He, L. Lin, S. Song, M. Xia, L. Xu, H. Ying, J. Chen, Mineralization of C.I. Reactive Blue 19 by ozonation combined with sonolysis: Performance optimization and degradation mechanism, Sep. Purif. Technol. 62 (2008) 376–381.
[14] Y.J. Acosta-Silva, R. Nava, V. Hernández-Morales, S.A. Macías-Sánchez, M.L. Gómez-Herrera, B. Pawelec, Methylene blue photodegradation over titania-decorated SBA-15, Appl. Catal. B: Environ. 110 (2011) 108–117.
[15] Y.J. Acosta-Silva, R. Nava, V. Hernández-Morales, S.A. Macías-Sánchez, B. Pawelec, TiO_2/DMS-1 disordered mesoporous silica system: Structural characteristics and methylene blue photodegradation activity, Microporous Mesoporous Mater. 170 (2013) 181–188.
[16] M. Ahmad, E. Ahmed, Z.L. Hong, J.F. Xu, N.R. Khalid, A. Elhissi, W. Ahmed, A facile one-step approach to synthesizing ZnO/graphene composites for enhanced degradation of methylene blue under visible light, Appl. Surf. Sci. 274 (2013) 273–281.
[17] M.R. Bayati, F. Golestani-Fard, A.Z. Moshfegh, Visible photodecomposition of methylene blue over micro arc oxidized WO_3–loaded TiO_2 nano-porous layers, Appl. Catal. A: Gen. 382 (2010) 322–331.
[18] A. Ghauch, A.M. Tuqan, N. Kibbi, S. Geryes, Methylene blue discoloration by heated persulfate in aqueous solution, Chem. Eng. J. 213 (2012) 259–271.
[19] J. Kasanen, J. Salstela, M. Suvanto, T.T. Pakkanen, Photocatalytic degradation of methylene blue in water solution by multilayer TiO_2 coating on HDPE, Appl. Surf. Sci. 258 (2011) 1738–1743.
[20] J.-Z. Kong, A.-D. Li, X.-Y. Li, H.-F. Zhai, W.-Q. Zhang, Y.-P. Gong, H. Li, D. Wu, Photo-degradation of methylene blue using Ta-doped ZnO nanoparticle, J. Solid State Chem. 183 (2010) 1359–1364.
[21] C. Lizama, J. Freer, J. Baeza, H.D. Mansilla, Optimized photodegradation of Reactive Blue 19 on TiO_2 and ZnO suspensions, Catal. Today 76 (2002) 235–246.
[22] W. Shen, Z. Li, H. Wang, Y. Liu, Q. Guo, Y. Zhang, Photocatalytic degradation for methylene blue using zinc oxide prepared by codeposition and sol–gel methods, J. Hazard. Mater. 152 (2008) 172–175.
[23] T.-Y. Wei, C.-Y. Kuo, Y.-J. Hsu, S.-Y. Lu, Y.-C. Chang, Tin oxide nanocrystals embedded in silica aerogel: Photoluminescence and photocatalysis, Microporous Mesoporous Mater. 112 (2008) 580–588.
[24] D. Zhao, G. Sheng, C. Chen, X. Wang, Enhanced photocatalytic degradation of methylene blue under visible irradiation on graphene@TiO_2 dyade structure, Appl. Catal. B: Environ. 111–112 (2012) 303–308.
[25] F. Abdelmalek, S. Gharbi, B. Benstaali, A. Addoum, J.L. Brisset, Plasmachemical degradation of azo dyes by humid air plasma: Yellow Supranol 4 GL, Scarlet Red Nylosan F3 GL and industrial waste, Water Res. 38 (2004) 2339–2347.
[26] J.-L. Brisset, D. Moussa, A. Doubla, E. Hnatiuc, B. Hnatiuc, G.K. Youbi, J.-M. Herry, M. Naïtali, M.-N. Bellon-Fontaine, Chemical reactivity of discharges and temporal post-discharges in plasma treatment of aqueous media: Examples of gliding discharge treated solutions, Ind. Eng. Chem. Res. 47 (2008) 5761–5781.
[27] J. Janča, A. Czernichowski, Wool treatment in the gas flow from gliding discharge plasma at atmospheric pressure, Surf. Coat. Technol. 98 (1998) 1112–1115.
[28] S. Laminsi, E. Acayanka, S. Nzali, P. Teke Ndifon, J.-L. Brisset, Direct impact and delayed post-discharge chemical reactions of Fe II complexes induced by non-thermal plasma, Desalin. Water Treat. 37 (2012) 38–45.
[29] J.-L. Brisset, J. Pawlat, Chemical effects of air plasma species on aqueous solutes in direct and delayed exposure modes: Discharge, post-discharge and plasma activated water, Plasma Chem. Plasma Process (2015) 1–27.
[30] J.-L. Brisset, E. Hnatiuc, Peroxynitrite: A re-examination of the chemical properties of non-thermal discharges burning in air over aqueous solutions, Plasma Chem. Plasma Process. 32 (2012) 655–674.